applied sciences

MDPI

Article

Dosimetric Evaluation of the Inter-Fraction Motion of Organs at Risk in SBRT for Nodal Oligometastatic Prostate Cancer

Francesco La Fauci [1,†], Matteo Augugliaro [2,‡], Giovanni Carlo Mazzola [2,3], Stefania Comi [1], Matteo Pepa [2,§], Mattia Zaffaroni [2], Maria Giulia Vincini [2,*], Giulia Corrao [2,3], Francesco Alessandro Mistretta [3,4], Stefano Luzzago [3,4], Cristiana Fodor [2], Gennaro Musi [3,4], Salvatore Gallo [5], Giuseppe Petralia [3,6], Ottavio De Cobelli [3,4], Roberto Orecchia [7], Federica Cattani [1,‖], Giulia Marvaso [2,3,‖] and Barbara Alicja Jereczek-Fossa [2,3,‖]

1 Unit of Medical Physics, IEO, European Institute of Oncology IRCCS, 20141 Milan, Italy
2 Division of Radiation Oncology, IEO, European Institute of Oncology IRCCS, 20141 Milan, Italy
3 Department of Oncology and Hemato-Oncology, University of Milan, 20122 Milan, Italy
4 Department of Urology, IEO, European Institute of Oncology IRCCS, 20141 Milan, Italy
5 Department of Physics "Aldo Pontremoli", University of Milan, 20133 Milan, Italy
6 Precision Imaging and Research Unit, Department of Medical Imaging and Radiation Sciences, IEO, European Institute of Oncology IRCCS, 20141 Milan, Italy
7 Scientific Directorate, IEO, European Institute of Oncology IRCCS, 20141 Milan, Italy
* Correspondence: mariagiulia.vincini@ieo.it
† Current address: Humanitas Research Hospital, 20089 Rozzano, Italy
‡ Current address: Radiation Therapy Unit, Azienda USL-IRCCS di Reggio Emilia, 42123 Reggio Emilia, Italy
§ Current address: Centro Nazionale di Adroterapia Oncologica (CNAO), 27100 Pavia, Italy
‖ Co-last authors.

Citation: La Fauci, F.; Augugliaro, M.; Mazzola, G.C.; Comi, S.; Pepa, M.; Zaffaroni, M.; Vincini, M.G.; Corrao, G.; Mistretta, F.A.; Luzzago, S.; et al. Dosimetric Evaluation of the Inter-Fraction Motion of Organs at Risk in SBRT for Nodal Oligometastatic Prostate Cancer. *Appl. Sci.* **2022**, *12*, 10949. https://doi.org/10.3390/app122110949

Academic Editor: Jan Egger

Received: 10 September 2022
Accepted: 24 October 2022
Published: 28 October 2022

Publisher's Note: MDPI stays neutral with regard to jurisdictional claims in published maps and institutional affiliations.

Copyright: © 2022 by the authors. Licensee MDPI, Basel, Switzerland. This article is an open access article distributed under the terms and conditions of the Creative Commons Attribution (CC BY) license (https://creativecommons.org/licenses/by/4.0/).

Abstract: In this paper, we aim to evaluate the entity of inter-fraction organ motion and deformation in stereotactic body radiotherapy (SBRT) treatments for nodal oligometastatic prostate cancer (PCa). Thirty-three patients with lymph nodes showing oligometastatic PCa treated with SBRT were included. Organs at risk (OARs) were delineated using both simulation computer tomography (s-CT) and daily cone beam CTs (CBCTs) using the Raystation planning system. For each OAR, the union volume (UV) between all the CBCTs and s-CT was computed. An expanded volume (EV) of the s-CT OARs was applied using six different margins (3, 5, 8, 10, 15, and 20 mm). A percentage volume (V%) was computed to assess the intersection between each EV and UV. The OAR deformation and motion were further evaluated using the dice similarity coefficient (DSC) and mean distance to agreement (Mean_DA). The percentage maximum dose variations for all the OARs were estimated. A recalculation with higher dose prescriptions was performed by prescribing 36 Gy/3 fx, as well as 45 Gy/3 fx. The cauda showed the highest matching (DSC = 0.72; Mean_DA = 0.14 cm), and the colon showed the lowest one (DSC = 0.37; Mean_DA = 0.44 cm). The minimum margin, which ensured a V% > 95%, was 3 mm (97.5%) for the cauda and 15 mm (96.6%) for the colon. All the OARs reached the compliance of the constraints in each session. Regarding 36 Gy-plans, the ileum punctual compliance Dmax failed in 58.8% of patients, and it failed in 70.6% of the patients for the ileum, 7.14% for the colon, and 12.5% for the bladder in the case of 45 Gy-plans. This study is an ancillary study of the RADIOSA clinical trial (AIRC IG-22159) and can be used as a benchmark for dose escalation.

Keywords: oligometastatic prostate cancer; stereotactic body radiotherapy; computed tomography; planning; inter fraction; organ motion

1. Introduction

Stereotactic body radiotherapy (SBRT) represents a non-invasive, ablative local treatment applied to several anatomical sites for both oligorecurrent and oligoprogressive cancer diseases, and it has become a particularly valuable treatment option for managing

oligometastatic prostate cancer (PCa) patients. In fact, although chemo-hormonal therapy represents the standard treatment for high-volume metastatic castration-sensitive PCa patients [1], no additional chemo-therapy treatment has demonstrated survival benefits for low-volume metastatic PCa [2]. Indeed, SBRT represents an emerging low-toxicity technique for oligometastasis [3]. In an oligometastatic PCa setting, considered as an intermediate phase of tumor spreading with a limited metastatic capacity (no more than five sites of the disease) [4,5], treating all the metastatic lesions with small-volume, high-dose SBRT can potentially eliminate all the macroscopic cancer foci, thereby achieving local control, extending progression-free survival (PFS), and improving the overall survival (OS) [6], with no relevant side effects [7,8]. Hence, SBRT treatment represents a valid instrument for achieving local control, delaying progression, and postponing the need for further treatment.

Despite these excellent results, SBRT is more affected by single daily uncertainty, since the total treatment error is not averaged over several daily sessions, as in conventional radiotherapy. In this scenario, the estimation of uncertainties during the entire treatment is mandatory so as to permit the evaluation of the delivery accuracy, the definition of the narrower margins, the comprehension of the surrounding organ displacement, and, consequently, the possibility of increasing the dose to the target volume without compromising the normal tissue function [9–11]. Advances in radiation therapy (RT) planning have led to the safe delivery of doses to tumors, improving local control and sparing healthy tissues, consequently improving patients' quality of life. A goal of all RT treatments is to deliver radiation to the target organs at volumes as close to the planned dose distribution as possible. However, delivery conditions, patient set-up, and internal anatomy represent uncertainties that can affect the treatment delivery accuracy. In particular, discrepancies can be due to inaccuracies in the patient positioning, intra- or inter-fraction organ motion, and volume variation (i.e., bowel displacement for abdominal pelvic lesions or bladder/rectum filling). As these modifications can impact the actual dose distribution and, consequently, the compliance with OAR constraints, the quantification of these variations and a high degree of accuracy are desirable.

In all RT treatments, it is possible to distinguish between two classes of errors that might affect the treatment quality: (i) the set-up errors, linked to the immobilization of the patient and accuracy of the imaging system, and (ii) inter- and intra-fraction errors, related to organ motion and the volume variability, which are independent of the set-up errors. Set-up errors are corrected using image-guided RT (IGRT) systems, which enable us to acquire patient's image in the treatment room immediately prior to irradiation and correct the tumor displacement and observe the simulation frame through couch rotation and translation. However, since the human body is not rigid, the inter- or intra-fraction errors, due to organ motion, deformation, shrinkage, and the filling status, cannot be corrected by the rationale of IGRT alone. Therefore, the expansion of the target structures (i.e., planning target volume, PTV) or OARs (i.e., planning risk volume, PRV) by the use of clinical margins has to be applied so as to consider such modifications. Thus, the second type of error is more critical, creating a different picture from the one used during the planning, and this work will focus on the inter-fraction variations in the abdominal and pelvic organs.

All these aspects need to be carefully considered, especially in the case of SBRT treatments. As a matter of fact, in SBRT, a relatively high irradiation dose is delivered in a limited number of fractions (fx) and in a highly conformal manner, resulting in steep dose gradients between the targets and OARs and minimizing the involvement of the nearby healthy structures. Thus, geometric and anatomical variations can have significant impacts [12–14].

The aim of this retrospective study is to evaluate the displacement of the main OARs involved in PCa SBRT treatment in view of a further dose escalation, and to the best of our knowledge, it is one of the first to include patients with lymph node oligometastases. In particular, this study focuses on colon and small intestine displacements and their

effects on the delivered dose by simulating the inter-fraction variations in the treatment planning system (TPS). This research is an ancillary study of the randomized phase II clinical trial RADIOSA (Radioablation With or Without Androgen Deprivation Therapy (ADT) in Metachronous Prostate Cancer OligometaStAsis) with the aim of comparing SBRT +/- ADT for oligorecurrent-castration-sensitive PCa (OCS-PCa) in terms of its efficacy, toxicity, and patient quality of life.

2. Methods

2.1. Patients and Inclusion Criteria

A retrospective study was conducted, including patients treated at our institute (European Institute of Oncology IRCCS—IEO, Milan, Italy), between May 2012 and December 2020 and was part of general SBRT and image-guided RT research reported to the Ethical Committee of the IEO (notifications 79/10, 86/11, 87/11, and 93/11). The inclusion criteria for the study were: (1) isolated oligometastatic PCa with abdominal-pelvic lymph node recurrence; (2) treatment with SBRT; and (3) written informed consent to receive SBRT.

The diagnosis of a clinically evident lymph node showing recurrent PCa was performed on the basis of biochemical progression and imaging studies, such as [11C], choline PET, prostate-specific membrane antigen positron emission tomography (PSMA-PET), and magnetic resonance imaging.

2.2. Simulation and Treatment Delivery

The immobilizing system used was Combifix (CIVCO radiotherapy, Orange City, Iowa), and all the patients were simulated in the head-first supine position with the arms positioned over the chest, without any specific pre-treatment preparation. All the plans were optimized and calculated with Iplannet (version 4.5.3 by BrainLab®) or Raystation (version 9B (Raysearch® Stockholm, Sweden). The plans were optimized to guarantee a coverage of 95% of the PTV volume by 95% of the prescribed dose and a maximum dose inferior to 110%. Timmerman's work [15], based the constraints for pelvic SBRT used in our institution, was utilized for the optimization. All the SBRT plans were delivered using the Vero system® (Mitsubishi-BrainLab). For each patient, IGRT with CBCT was conducted just before every fraction to enable the daily pretreatment positioning verification and online correction of set-up errors.

2.3. Data Processing, Image Registration, and Contouring of Structures of Interest

To ensure their compatibility with the software used for the further analyses (i.e., RayStation®), the daily CBCTs were converted from their native format, a combination of RAW images and TXT files containing their DICOM tags, into the standard DICOM format using an in-house algorithm developed with MATLAB version R2020b (MathWorks®). The script allowed us to merge and normalize the imaging data stored on the RAW file, as well as the DICOM information present in the TXT file, into one single DICOM file. All the Iplannet® plans and daily CBCTs were then imported into Raystation®.

A rigid registration between the simulation CT (s-CT) (CT Optima 580, General Electric Healthcare, (2.5 mm slice thickness) and each daily CBCT (1 mm slice thickness) was performed. The registration was based firstly on the bony anatomy and secondly on the gross tumor volume (GTV) in order to reproduce the condition of the target verification position at the time of treatment, and the position was corrected for the translation, pitch, and roll direction through the robotic couch. The delineation of the GTV, planning target volume (PTV) (margins of 3 mm or 5 mm), and OARs for each patient was performed using the s-CT and each daily CBCT to observe the volume variations of the structures and evaluate geometric discrepancies due to their deformation during the treatment (inter-fraction variability). The contouring was performed by the

same radiation oncologist for both the s-CTs and CBCTs in order to avoid inter-observer variability [16], according to the RTOG guidelines.

As far as the colon and ileum were concerned, only the intestinal loop closest to the target was contoured. Since the field of view of the Vero system was smaller than that of the CT (20 cm vs. 65 cm diameter), only the OARs visible in their entirety were outlined in the daily CBCTs.

2.4. Volume Similarity Indexes

All the structures delineated on the rigidly registered CBCTs were transferred to the reference s-CT. The evaluation of the volume variability, comparing each OAR in each CBCT with the corresponding one on s-CT, was estimated using the ROI_comparison algorithm implemented on Raystation, exploiting the dice similarity coefficient (DSC) and the mean distance to agreement (Mean_DA). These validated metric parameters [17,18] were selected in accordance with the American Association of Physicists in Medicine (AAPM Task Group 132) [19]. The *DSC* is defined as:

$$DSC = 2 \times \frac{A \cap B}{A + B}$$

where *A* and *B* are two different contours referring to the same OAR. The closer the output value is to 1, the higher the overlap and correspondence between the structures are. This index was used to calculate the similarity between structures. Additionally, the structure's relative distance was estimated through the mean distance to agreement (Mean_DA) [19]. The Mean_DA is a geometrical parameter defined as the mean distance that each point on the A contour of s-CT would have to travel in order to overlap with the nearest point on the contour B of the same structure on the daily CBCT. For each patient and each available CBCT, the DSC and Mean_DA indexes were evaluated for each OAR and compared to the reference structure in s-CT. The identification of potential outliers in the DSC and Mean_DA populations was performed graphically using a box plot.

Regarding spherical-like structures, such as the bladder, the difference between the center of mass (COM) of the structure contoured in the reference s-CT and in each CBCT was also considered in order to quantify the organ displacement [20]. This was possible via the Raystation tool Localize ROI. The mean displacement of the COM in all the directions was calculated, as well as the relative error, calculated as the standard deviation.

2.5. Evaluation of the Volume Variation

The OARs delineated on the reference s-CT were considered as reference structures and were isotropically expanded to obtain the so-called expanded volume (EV) using 6 margins: 3 mm, 5 mm, 8 mm, 10 mm, 15 mm, and 20 mm [16].

For each patient, a union volume (UV) was created for each OAR by considering the Boolean union between the reference structure on the s-CT and the same structure on all the available CBCTs. Then, the intersections between the UV and each of the 6 EVs were computed, obtaining 6 intersection volumes (IV) for each OAR.

The structure of the s-CT was included in order to consider the entire displacement of the OAR from the s-CT, which represents the delivered plan, to the daily treatment session (CBCT).

Afterward, the probability of enveloping the structure's displacement during treatment was expressed by the percentage volume (*V*%) of each IV with respect to the UV, which was calculated as:

$$V\% = \frac{IV}{UV} \times 100$$

The margin corresponding to *V*% > 95% was considered a conservative estimate of the margin necessary to take the organ motion into account [16] during the entire treatment. For each structure, the *V*% > 95% and the corresponding margin were calculated. For those patients whose *V*% was not able to achieve the 95% threshold, the margin cor-

responding to the highest *V*% was considered. The optimal margin required for each organ to take its motion into account was defined by evaluating the median margin corresponding to *V*% > 95% (or the greatest) for all the patients. Since each structure presented with a population lower than 20 samples, with an asymmetrical data distribution, the median value was considered a good estimation parameter for the optimal margin definition. A schematic representation of the workflow and the involved volumes can be seen in Figure 1 and Figure 2, respectively.

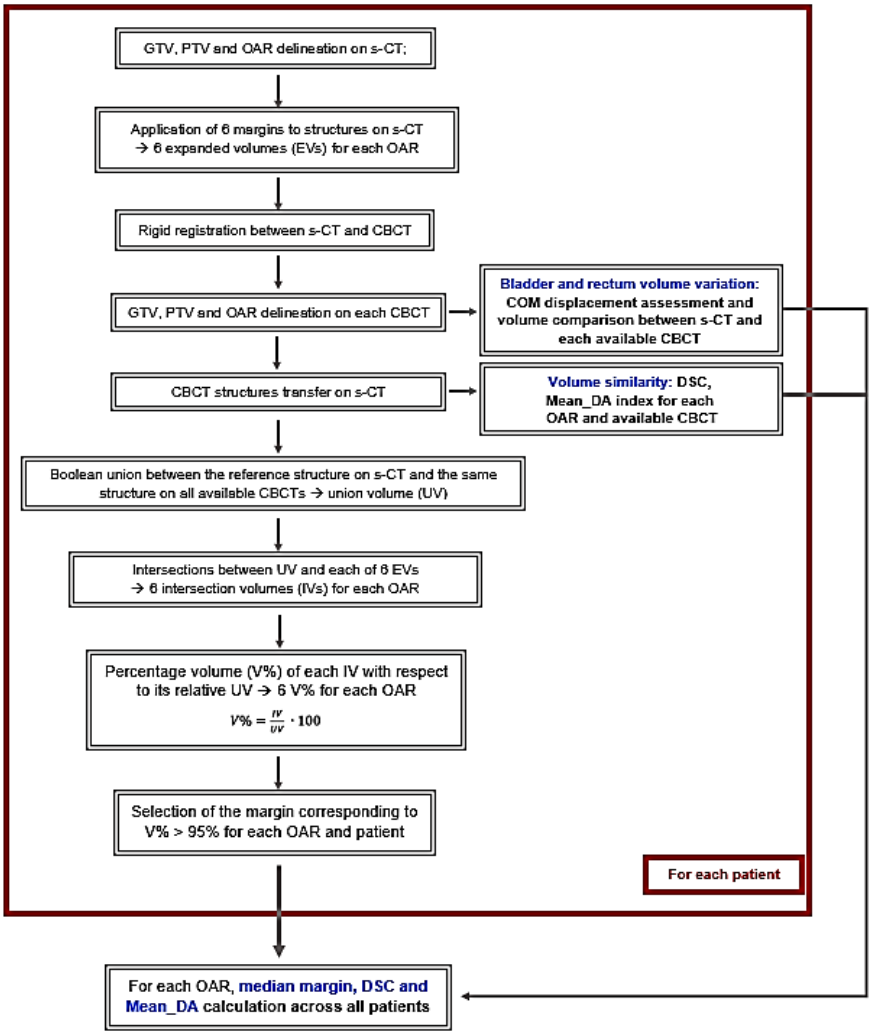

Figure 1. A schematic workflow of the methods.

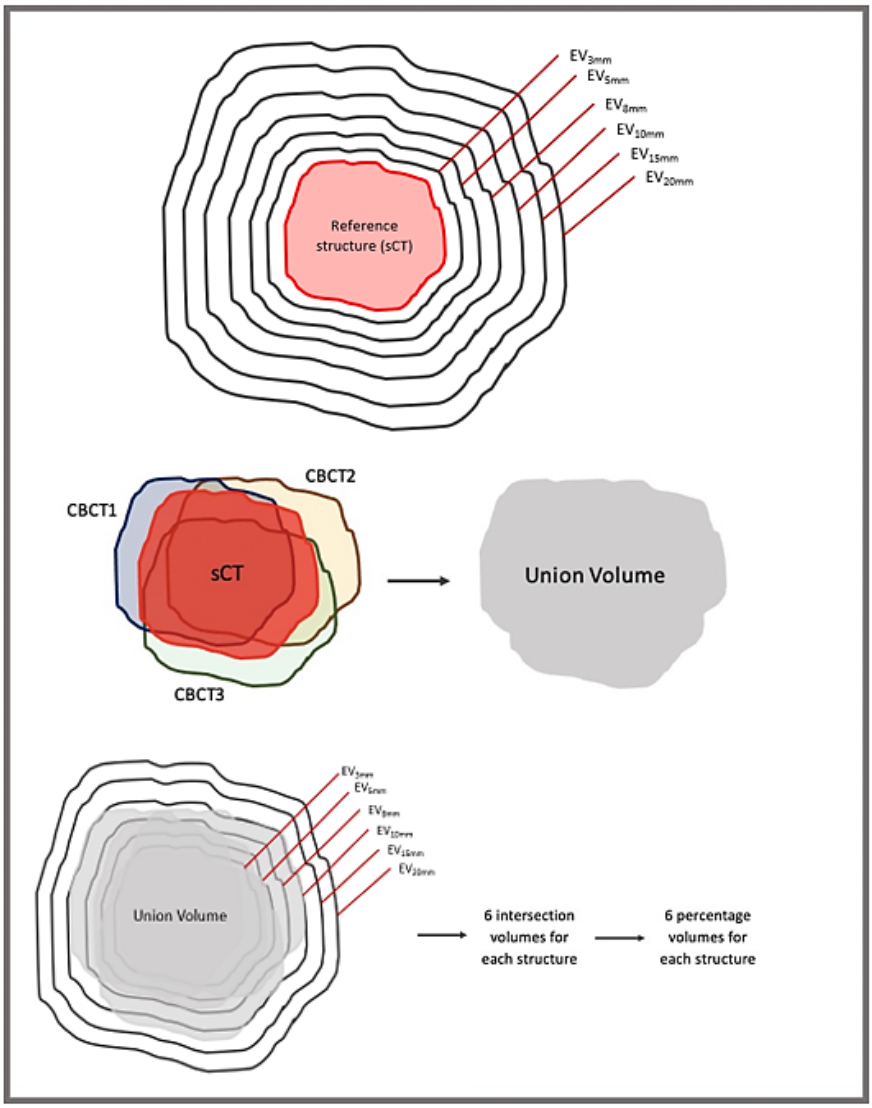

Figure 2. Schematic representation of the 6 expanded volumes (**top**), creation of the union volume between the s-CT and CBCT structures (**center**), and creation of the 6 intersection volumes (and, consequently, 6 percentage volumes), superimposing the union volume onto each of the 6 expanded volumes (**bottom**).

With regard to the bladder and rectum, in order to include not only the volume variation due to the organ motion but also the deformation and variability due to the filling and emptying status, the differential variations in the daily volume (V_day), with respect to the reference volume (V_ref), on the s-CTs were evaluated [21]. For every structure, the mean volume on the available CBCTs was calculated for each patient, and differences between the populations of data and the corresponding volumes on the s-CTs were assessed using Wilcoxon signed-rank tests. In addition, the median volume on the s-CTs and CBCTs were calculated for all the patients. As in the case of the DSC and Mean_DA, a box plot analysis was performed for each structure's volume.

2.6. Effect on the Dose

The effect of the OAR displacement on the dose distribution was estimated by evaluating the variation in the maximum dose (Dmax) for each OAR. The actual delivered plans were recalculated based on the s-CTs with the structures from each CBCT, and the

percentage Dmax variations were evaluated. Dmax was chosen as the most representative parameter for the daily dose variation, since all the other dose–volume histogram (DVH) indexes presented values considerably below the constraints used in Folkert et al. [15]. As was performed for the volume variations, for every structure, the mean Dmax based on the available CBCTs was calculated for each patient, and differences between the populations of data and the corresponding volumes on the s-CTs were assessed using the Wilcoxon signed-rank test. In addition, the median Dmax on the s-CTs and CBCTs were calculated for all the patients.

In addition, recalculations of the delivered plans with higher dose prescriptions, without re-optimization, were performed by prescribing 36 Gy/3 fx, as well as 45 Gy/3 fx, for further dose escalation studies. Since no re-optimization process was considered, the recalculation merely consisted of a voxel re-scaling of the original dose distribution.

3. Results

Thirty-three patients met the inclusion criteria and were included in the study. Thirty-one (94%) of them received 21 to 30 Gy in 3 fx, while the other two (6%) received 25 Gy in 5 and 32 Gy in 4 fx, and a total amount of 135 CTs was collected. In total, 9.7% of the patients were treated with intensity-modulated RT (IMRT), 80.4% with conformal dynamic arc (CDA), and 9.7% with dynamic wave arc (DWA).

3.1. Margin Assignment and Structure Deformation Characterization

For each considered structure, the values of the median similarity index DSC, median Mean_DA, median V%, and median margin are displayed in Table 1. The cauda, as expected, showed the lowest value of both the Mean_DA and margin and the highest DSC. A more critical scenario was presented both by the ileum and colon, where margins of 10 mm and 15 mm, respectively, were needed, and low DSC and high Mean_DA values were reached. The DSC and Mean_DA box plots are presented in Figure 3. These results revealed the static nature of the cauda, since it was not affected by mechanical stress, displacement, or a high degree of deformation, in contrast to the OARs, such as the ileum and colon. The bladder and rectum reached a DSC index near 0.7 and, hence, presented a smaller shape variability, although they showed a greater Mean_DA and margin (8 mm) with respect to the cauda. The numbers of patients reaching a V% ≥ 95% with respect to each of the six considered margins are presented in Table 2.

Table 1. From left to right: the OAR considered, median DSC, median Mean_DA, median V%, and median optimal margin for all the patients.

OAR	Median DSC	Median Mean_DA (cm)	Median V%	Median Optimal Margin (mm)
Cauda	0.72	0.14	97.47	3
Bladder	0.70	0.43	97.02	8
Rectum	0.68	0.33	95.39	8
Ileum	0.50	0.38	95.86	10
Colon	0.37	0.44	96.60	15

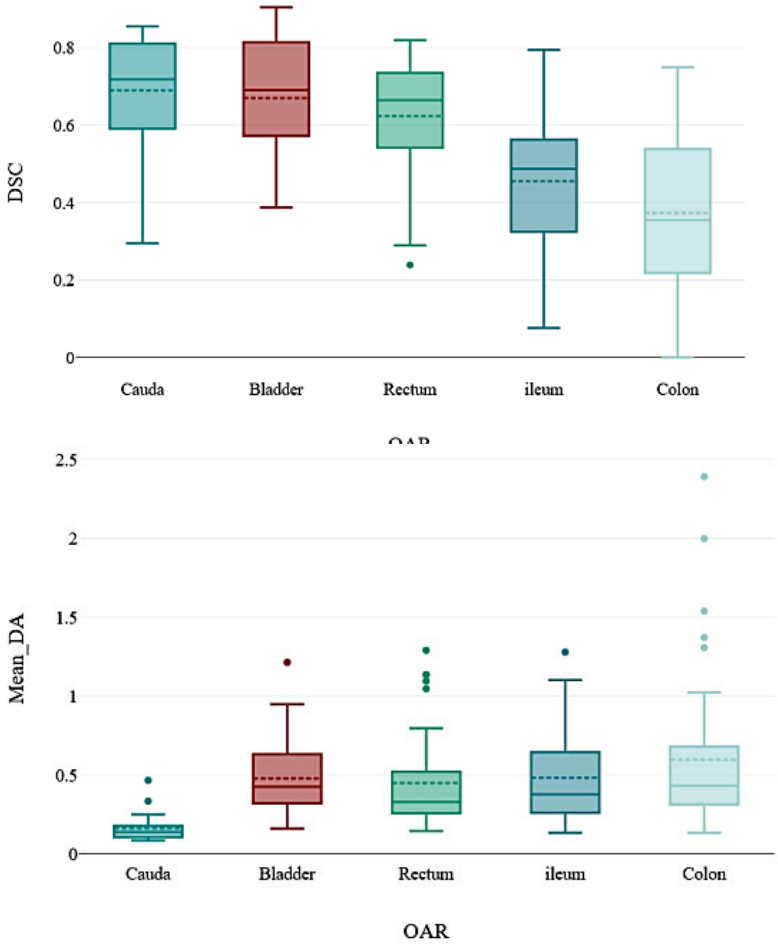

Figure 3. DSC (**top**) and Mean_DA (**bottom**) distributions for all the considered organs.

Table 2. Number of patients whose V% was greater than 95% with each of the 6 considered margins.

OAR (total # of Patients)		Margin (mm)					
		3	5	8	10	15	20
Cauda (9)	#	6	8	9			
	%	66.67	88.89	100.00			
Rectum (17)	#	2	4	9	12	13	13
	%	11.76	23.53	52.94	70.59	76.47	76.47
Bladder (9)	#	2	2	6	6	8	8
	%	22.22	22.22	66.67	66.67	88.89	88.89
Ileum (20)	#	0	3	9	12	14	18
	%	0.00	15.00	45.00	60.00	70.00	90.00
Colon (15)	#	0	1	5	6	10	12
	%	0.00	6.67	33.33	40.00	66.67	80.00

3.2. Volume Variation

The median and mean of the V% variation regarding the volumes on the s-CTs and CBCTs are reported in Table 3 for each structure. Wilcoxon's signed-rank test did not show any significant difference between the volumes on the s-CTs and CBCTs for every structure, with the exception of the bladder. Box plots regarding the volume variations are presented in Figure 4 for each OAR. The cauda showed the lowest volume variation, as expected. As far as the bladder and rectum are concerned, the V% variations, calculated as the percentage variation in the daily volume with respect to V_ref, presented a random variation trend in all of the CBCTs were evaluated (see Supplementary Materials, Figures S1 and S2). The bladder mean COM displacement results were (−3.71 ± 0.86) mm, (0.25 ± 0.30) mm, and (1.32 ± 0.46) mm in the inferior–superior, left–right, and anterior–posterior directions, respectively.

Table 3. From left to right: the OAR considered, median CBCT, median s-CT, and median variation values of the volume for all the patients.

OAR	Median s-CT Volume (Range) (cc)	Median CBCT Volume (Range) (cc)	Median Volume Variation (%)
Cauda	12.54 (3.17–30.72)	12.76 (2.81–27.96)	−9.51
Bladder	72.03 (44.08–247.42)	71.29 (24.96–168.39)	−5.55
Rectum	45.72 (7.32–98.01)	44.61 (5.6–145.21)	−9.82
Ileum	22.04 (6.6–157.38)	24.6 (3.22–148.06)	3.79
Colon	17.58 (8.76–74.97)	16.47 (2.82–124.76)	−16.89

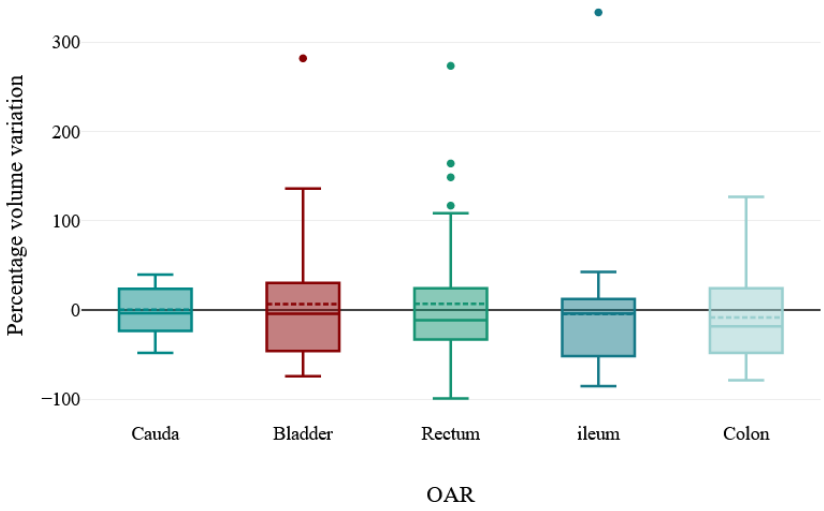

Figure 4. Percentage volume variation distributions for all the considered organs.

3.3. Dosimetric Constraint Compliance and Dose Variation

Since all the constraints were highly respected in all the s-CT plans, the Dmax percentage variation was selected for the estimation of the daily dose variation in the case of the OARs. In Table 4, the median Dmax and Dmax percentage variations in the s-CTs and CBCTs for every OAR are shown. No statistically significant variations between the Dmax values on the s-CTs and on CBCTs were detected for all the OARs. Regarding the recalculation with the higher dose prescription, the 36 Gy-plans failed for the ileum punctual

Dmax in 58.8% of the patients in all the treatment sessions, and 45 Gy-plans failed in 70.6% of the patients for the ileum, 7.14% for the colon, and 12.5% for the bladder.

Table 4. From left to right: the OAR considered, median CBCT, median s-CT, and median CBCT values of Dmax for all the patients.

OAR	Median s-CT Dmax (Range) (Gy)	Median CBCT Dmax (Range) (Gy)	Median Dmax Variation (%)
Cauda	5.54 (0.55–7.32)	5.66 (0.47–7.32)	−1.87
Bladder	11.14 (0.62–19.55)	5.89 (0.53–23.20)	−20.09
Rectum	14.57 (0.45–30.14)	13.90 (2.96–30.51)	−4.11
Ileum	22.19 (5.97–29.62)	20.31 (6.04–31.90)	−1.38
Colon	11.32 (8.8–30.21)	13.85 (4.97–30.37)	−3.00

4. Discussions

This study is an ancillary study of the RADIOSA trial (AIRC IG-22159) with the aim of investigating and characterizing the entity of the OAR motion due to shrinkage, displacement, and volume variation related to the filling or emptying status of the organs during SBRT treatment. Despite significant volume variations under the influence of the organ motion, the impact on the dose is only modest in terms of the constraint compliance, with a good level of local control and toxicity profile.

Although several studies on OAR motion in the hypo-fractionated treatment of primitive prostate tumors are available in the literature [22–26], to the best of our knowledge, none of them explored organ movement in patients with lymph node oligometastatic PCa.

The first section of this work focused on the assessment of the variability in the OAR structures between the s-CTs and daily CBCTs in order to identify volume variations, displacement, deformation, and shrinkage, playing important roles in the definition of a good treatment delivery.

The colon and ileum were found to be the most critical OARs, as we demonstrated that they needed a margin of 15 mm and 10 mm, respectively, to reach the 95% V% threshold. This variability can be ascribed to the very mutable shape of these organs, which is related to their physiological activity. Indeed, it is very well known that the small bowel is subjected to several mechanical stresses, which strongly affect the shape and entity of the movements of the organ itself [27–29]. On this basis, the isotropic margin was adopted.

A comparable entity displacement in the case of the ileum was observed by Nuyttens et al. [29] in patients receiving adjuvant pelvic RT for rectal cancer. Nonetheless, the main difference from our study was the modality of the displacement estimation. Nuyttens et al. [29] measured the absolute length by considering the fixed point of reference in the bony anatomy, estimating the distance between certain predefined points in the spine and other chosen points in the small bowel. Instead, the entity of displacement in our work was computed as the relative distance between the surface of the structure in the s-CT and in the CBCT. A similar recent study by Cuccia et al. [30] observed a similar trend in terms of the volume variation and Dmax for the bowel and, analogously with our study, inter-observer variability was avoided by enrolling one physician to contour all the OARs of interest. Concerning the bladder and rectum, their anatomical differences can be mainly related to their filling status. Regarding the rectum displacement, our results are comparable with those of Nuyttens et al. [31] and Njikamp et al. [32] (>10 mm). Similar values were also reported by Brierley et al. [33], who derived margins of 8–9 mm for the displacement of the rectum. A displacement greater than 10 mm was observed by Yamashita et al. [34], who concluded that margins of up to 10–15 mm are sufficient for identifying rectum movement.

For the rectal volume variation, Li et al. [21] observed lower values in a range between −50.4% and 47.3% among PCa patients, and the authors concluded that this variation was due to the difficulty experienced by the patient in following the instructions for the correct rectal preparation. The patients in our study did not need to receive any preparation, since their lymph nodal metastases were treated, so that the percentage volume variations due to the different emptying statuses were even more pronounced (ranging from −99.2% up to 273.6%).

Regarding the bladder volume variation, similar results were shown by Li et al. [21], reporting a variation range between −79.7% and 203.0%, in line with the findings of this study, with variations ranging from −74.2% up to 282.0%. In Byun et al. [20], a lower mean displacement value for the bladder was shown regarding the lateral direction and anterior/posterior and inferior/superior directions, with displacements of 0.02 ± 2.90, −0.86 ± 6.24, and −3.40 ± 8.80 mm, respectively.

Both Li et al. [21] and Byun et al. [23] considered patients with a full bladder and empty rectum. On the contrary, the differences reported in the present study are more marked, since the patients did not follow any instruction, as mentioned before.

Regarding the cauda, the reference structure defined in order to validate our methodology was not affected by deformation and shrinkage, and a margin of only 3 mm was required to achieve the percentage volume of 97%, and the highest DSC value was observed, corroborating its static status. The discrepancies are mainly due to the contour shape and structure length variability between the s-CTs and CBCTs. Regarding the dosimetric impact of the volume variation, we observed a high degree of compliance with the constraints adopted by our institute. In general, a greater percentage dose variation was observed, with higher Mean_DA values and smaller DSC values (see Supplementary Materials: Figure S3). Reasonably, the closer the DSC index is to 1 (two volumes perfectly overlapped,) the smaller the Mean_DA value is, and the smaller the dose percentage variations are (clearly observed in the bladder and colon). The observed deviation did not show a predictable drift during the treatment course.

As for the bladder and rectum, the volume variations are due to their expansion or contraction, caused by variations in their filling status [20,21]. Moreover, the rectum is more sensitive to variation in the shape of the anterior wall, as reported by Chong et al. [35] for rectal cancer patients. The colon and ileum presented with pronounced daily shape variation due to deformation caused by mechanical stress, as highlighted by their low median DSC and high median Mean_DA within a very wide interval range (see Figure 3). Moreover, as emerged from the box plots, the rectum, ileum, and colon are more affected by outliers, a fact that may be linked to the random nature of their shape variation. Regarding the cauda, these effects are not evident, since it is the structure with the smallest range interval for both the DSC and Mean_DA (contouring variability).

The main limitation of this study is related to the CBCT image quality. In fact, it is common knowledge from the literature that images produced by a fan beam CT (as CT OPTIMA) have a superior quality in terms of their clarity, uniformity, anatomical accuracy, and contrast resolution [33] compared to CBCT [36–40].

Therefore, the main difficulty was related to the fact that were dealing with nosier images and artefacts, which may have particularly undermined the delineation of the ileum and colon. The inter-observer variability was negligible, as only one physician was enrolled to contour all the OARs of interest. For this reason, the colon and ileum presented a lower median DSC with respect to the cauda. Another limit is related to the absence of immobilization devices and preparation pre-treatment for the bladder and rectum, resulting in a greater volume variability related to their filling/emptying status. In addition, since the treatment times using the Vero system are rapid enough (with a beam-on time of less than 3 min), the intra-fraction variability was not considered. Furthermore, in this work, the relative distance between the structure's surfaces was considered, though not with respect to the target surface, since the registration between the s-CT and CBCT was performed with respect to the same reference frame system of the CTV. Moreover, the

CBCT structures were transferred rigidly to s-CT, whereupon the dose calculation was performed. This modality was preferred to the daily dose calculation based on the CBCT, since the Dmax values of all the OARs were much lower (ranging from 20% to 40%, corresponding to 5–10 Gy) than the constraints used [15,22] for all the approved plans delivered (21 Gy/3 fx, 30 Gy/3 fx, 25 Gy/5 fx, and 32 Gy/4 fx). The recalculation of the plans on CBCT would have been more affected by the small FOV, presence of artefacts, inadequate Hounsfield unit (HU) calibration, and bad image quality rather than the HU variations in the structures over each session. Despite the abovementioned limitations, the study characterized the entity of the volume variability and structure displacement, demonstrating the safety of the delivered treatment. Indeed, all the OARs showed constraint compliance in all the daily sessions, since all the volume–dose constraints were highly respected. Non-compliance with the constraints was observed only for the recalculated plans when simulating a higher dose prescription, in which the margins for the OARs were not considered during the optimization. As for the higher dose prescription setting, whether using these margins to generate a PRV can still generate an optimal plan without compromising the coverage, or whether it is more cost-effective to perform the plan adaptation in the case of an observed large organ variability, are still open questions, and further studies are needed.

5. Conclusions

The aim of the present research was to estimate and characterize the entity of the displacement and deformation of the OARs surrounding the pelvic lymph node target in each treatment session with respect to the s-CT. The study showed that there is no direct relationship between the entity of the displacement of the ileum/colon and the anatomical area treated. The median displacements evaluated were 0.38 cm and 0.44 cm, respectively.

These OARs resulted in the most critical structures, showing different geometrical shapes for every daily treatment fraction due to organ motion and deformation. Instead, regarding the bladder and rectum, the shape variability was mainly linked to the different daily filling and emptying statuses.

As previously mentioned, the work is an ancillary study of the RADIOSA trial (AIRC IG-22159) and can be used as a benchmark for analyzing the prospective results from the trial. Based on these considerations, a further investigation must be made in order to consider the possibility of dose escalation with respect to the re-optimization of the treatment plans, exploiting the selected optimal margins for each OAR with a higher dose prescription of 45 Gy/3 fx, evaluating the constraint compliance, and paving the way for dose escalation studies.

Supplementary Materials: The following supporting information can be downloaded at: https://www.mdpi.com/article/10.3390/app122110949/s1. Figure S1: Bladder percentage volume variation for each available CBCTs (1 to 5); Figure S2: Rectum percentage volume variation express as ((V_daily-Vref)/Vref)*100 for each available CBCTs (1 to 5); Figure S3: Percentage dose varation vs Mean_DA and DSC for each OAR. The dose percentage variation increases with increasing Mean_DA, and decreases with higher values of DSC.

Author Contributions: Conceptualization: F.L.F., G.M. (Giulia Marvaso), G.C. and B.A.J.-F.; methodology: F.L.F., G.M. (Giulia Marvaso), G.C. and B.A.J.-F.; software: F.L.F. and M.P.; validation: G.M. (Giulia Marvaso), F.C. and S.C.; formal analysis: F.L.F. and M.G.V.; investigation: F.L.F., M.A., G.C.M., C.F. and S.C.; data curation: F.A.M., S.L., S.G. and O.D.C.; writing—original draft preparation: F.L.F., M.G.V., M.P. and M.Z.; writing—review and editing: G.M. (Gennaro Musi), G.P., F.C., R.O., B.A.J.-F. and S.G.; visualization: M.G.V.; supervision: B.A.J.-F., G.M. (Gennaro Musi), G.P., F.C. and R.O. All authors contributed to manuscript's revision and read and approved the submitted version. All authors have read and agreed to the published version of the manuscript.

Funding: F.L.F., M.A., M.Z. and M.G.V. were supported by a research fellowship from the Associazione Italiana per la Ricerca sul Cancro (AIRC), entitled "Radioablation ± hormonotherapy for prostate cancer oligorecurrences (RADIOSA trial): potential of imaging and biology", registered at ClinicalTrials.gov NCT03940235 and approved by the Ethics Committee of IRCCS, Istituto Europeo

di Oncologia and Centro Cardiologico Monzino (IEO-997). IEO, the European Institute of Oncology, is partially supported by the Italian Ministry of Health (through the "Ricerca Corrente" and "5x1000" funds) and by an institutional grant from Accuray Incorporated, Medical Equipment Manufacturing, Sunnyvale, CA, USA.

Institutional Review Board Statement: The study was part of general SBRT and image-guided RT research reported to the Ethical Committee of the IEO (notifications 79/10, 86/11, 87/11, and 93/11).

Informed Consent Statement: Written informed consent to publish this paper was obtained from the patients.

Data Availability Statement: Not applicable.

Conflicts of Interest: B.A.J.F. received research funding from Accuray, AIRC (Italian Association for Cancer Research), Fondazione IEO-CCM (Istituto Europeo di Oncologia-Centro Cardiologico Monzino), and FUV (Fondazione Umberto Veronesi), Speakers fees were obtained from Roche, Bayer, Janssen, Carl Zeiss, Ipsen, Accuray, Astellas, Ferring, Elekta, and IBA, and consultation fees were obtained from Bayer, Janssen, Ipsen, and Astra Zeneca. The remaining authors declare no conflict of interest that are relevant to the content of this article.

References

1. James, N.D.; Sydes, M.R.; Clarke, N.W.; Mason, M.D.; Dearnaley, D.P.; Spears, M.R.; Ritchie, A.W.S.; Parker, C.C.; Russell, J.M.; Attard, G.; et al. Addition of docetaxel, zoledronic acid, or both to first-line long-term hormone therapy in prostate cancer (STAMPEDE): Survival results from an adaptive, multiarm, multistage, platform randomised controlled trial. *Lancet* **2016**, *387*, 1163–1177. https://doi.org/10.1016/s0140-6736(15)01037-5.
2. Gravis, G.; Boher, J.-M.; Chen, Y.-H.; Liu, G.; Fizazi, K.; Carducci, M.A.; Oudard, S.; Joly, F.; Jarrard, D.M.; Soulie, M.; et al. Burden of Metastatic Castrate Naive Prostate Cancer Patients, to Identify Men More Likely to Benefit from Early Docetaxel: Further Analyses of CHAARTED and GETUG-AFU15 Studies. *Eur. Urol.* **2018**, *73*, 847–855. https://doi.org/10.1016/j.eururo.2018.02.001.
3. Tree, A.C.; Khoo, V.S.; Eeles, R.A.; Ahmed, M.; Dearnaley, D.P.; Hawkins, M.A.; Huddart, R.A.; Nutting, C.M.; Ostler, P.J.; van As, N.J. Stereotactic body radiotherapy for oligometastases. *Lancet Oncol.* **2013**, *14*, e28–e37. https://doi.org/10.1016/s1470-2045(12)70510-7.
4. Hellman, S.; Weichselbaum, R.R. Oligometastases. *JCO* **1995**, *13*, 8–10.
5. Lievens, Y.; Guckenberger, M.; Gomez, D.; Hoyer, M.; Iyengar, P.; Kindts, I.; Romero, A.M.; Nevens, D.; Palma, D.; Park, C.; et al. Defining oligometastatic disease from a radiation oncology perspective: An ESTRO-ASTRO consensus document. *Radiother. Oncol.* **2020**, *148*, 157–166. https://doi.org/10.1016/j.radonc.2020.04.003.
6. Palma, D.A.; Olson, R.; Harrow, S.; Gaede, S.; Louie, A.V.; Haasbeek, C.; Mulroy, L.; Lock, M.; Rodrigues, P.G.B.; Yaremko, B.P.; et al. Stereotactic ablative radiotherapy versus standard of care palliative treatment in patients with oligometastatic cancers (SABR-COMET): A randomised, phase 2, open-label trial. *Lancet* **2019**, *393*, 2051–2058. https://doi.org/10.1016/s0140-6736(18)32487-5.
7. Ost, P.; Reynders, D.; Decaestecker, K.; Fonteyne, V.; Lumen, N.; De Bruycker, A.; Lambert, B.; Delrue, L.; Bultijnck, R.; Claeys, T.; et al. Surveillance or Metastasis-Directed Therapy for Oligometastatic Prostate Cancer Recurrence: A Prospective, Randomized, Multicenter Phase II Trial. *J. Clin. Oncol.* **2018**, *36*, 446–453. https://doi.org/10.1200/jco.2017.75.4853.
8. Shahi, J.; Poon, I.; Ung, Y.C.; Tsao, M.; Bjarnason, G.A.; Malik, N.H.; Zhang, L.; Louie, A.V.; Cheung, P. Stereotactic Body Radiation Therapy for Mediastinal and Hilar Lymph Node Metastases. *Int. J. Radiat. Oncol.* **2021**, *109*, 764–774. https://doi.org/10.1016/j.ijrobp.2020.10.004.
9. Sogono, P.; Bressel, M.; David, S.; Shaw, M.; Chander, S.; Chu, J.; Plumridge, N.; Byrne, K.; Hardcastle, N.; Kron, T.; et al. Safety, Efficacy, and Patterns of Failure After Single-Fraction Stereotactic Body Radiation Therapy (SBRT) for Oligometastases. *Int. J. Radiat. Oncol.* **2020**, *109*, 756–763. https://doi.org/10.1016/j.ijrobp.2020.10.011.
10. Wilke, L.; Andratschke, N.; Blanck, O.; Brunner, T.B.; Combs, S.E.; Grosu, A.L.; Moustakis, C.; Schmitt, D.; Baus, W.W.; Guckenberger, M. ICRU report 91 on prescribing, recording, and reporting of stereotactic treatments with small photon beams: Statement from the DEGRO/DGMP working group stereotactic radiotherapy and radiosurgery. *Strahlenther. Onkol.* **2019**, *195*, 193–198.
11. Wong, A.; Pitroda, S.; Watson, S.; Son, C.; Das, L.; Uppal, A.; Oshima, G.; Stack, M.; Khodarev, N.; Salama, J.; et al. Long-term Survivors of an SBRT Dose-Escalation Study for Oligometastases: Clinical and Molecular Markers. *Int. J. Radiat. Oncol.* **2015**, *93*, S64. https://doi.org/10.1016/j.ijrobp.2015.07.152.
12. Ahmed, K.A.; Barney, B.M.; Davis, B.J.; Park, S.S.; Kwon, E.D.; Olivier, K.R. Stereotactic body radiation therapy in the treatment of oligometastatic prostate cancer. *Front. Oncol.* **2013**, *2*, 215. https://doi.org/10.3389/fonc.2012.00215.
13. Berkovic, P.; De Meerleer, G.; Delrue, L.; Lambert, B.; Fonteyne, V.; Lumen, N.; Decaestecker, K.; Villeirs, G.; Vuye, P.; Ost, P. Salvage Stereotactic Body Radiotherapy for Patients With Limited Prostate Cancer Metastases: Deferring Androgen Deprivation Therapy. *Clin. Genitourin. Cancer* **2013**, *11*, 27–32. https://doi.org/10.1016/j.clgc.2012.08.003.

14. Schick, U.; Jorcano, S.; Nouet, P.; Rouzaud, M.; Vees, H.; Zilli, T.; Ratib, O.; Weber, D.C.; Miralbell, R. Androgen deprivation and high-dose radiotherapy for oligometastatic prostate cancer patients with less than five regional and/or distant metastases. *Acta Oncol.* **2013**, *52*, 1622–1628. https://doi.org/10.3109/0284186x.2013.764010.
15. Folkert, M.R.; Timmerman, R.D. Stereotactic ablative body radiosurgery (SABR) or Stereotactic body radiation therapy (SBRT). *Adv. Drug Deliv. Rev.* **2017**, *109*, 3–14. https://doi.org/10.1016/j.addr.2016.11.005.
16. Maggiulli, E.; Fiorino, C.; Passoni, P.; Broggi, S.; Gianolini, S.; Salvetti, C.; Slim, N.; Di Muzio, N.G.; Calandrino, R. Characterisation of rectal motion during neo-adjuvant radiochemotherapy for rectal cancer with image-guided tomotherapy: Implications for adaptive dose escalation strategies. *Acta Oncol.* **2011**, *51*, 318–324. https://doi.org/10.3109/0284186x.2012.666358.
17. Dice, L.R. Measures of the Amount of Ecologic Association Between Species. *Ecology* **1945**, *26*, 297–302. https://doi.org/10.2307/1932409.
18. Harms, W.B.; Low, D.A.; Wong, J.W.; Purdy, J.A. A software tool for the quantitative evaluation of 3D dose calculation algorithms. *Med. Phys.* **1998**, *25*, 1830–1836. https://doi.org/10.1118/1.598363.
19. Brock, K.K.; Mutic, S.; McNutt, T.R.; Li, H.; Kessler, M.L. Use of image registration and fusion algorithms and techniques in radiotherapy: Report of the AAPM Radiation Therapy Committee Task Group No. 132. *Med. Phys.* **2017**, *44*, e43–e76. https://doi.org/10.1002/mp.12256.
20. Byun, D.J.; Gorovets, D.J.; Jacobs, L.M.; Happersett, L.; Zhang, P.; Pei, X.; Burleson, S.; Zhang, Z.; Hunt, M.; McBride, S.; et al. Strict bladder filling and rectal emptying during prostate SBRT: Does it make a dosimetric or clinical difference? *Radiat. Oncol.* **2020**, *15*, 239.
21. Li, W.; Vassil, A.; Godley, A.; Mossolly, L.M.; Shang, Q.; Xia, P. Using daily diagnostic quality images to validate planning margins for prostate interfractional variations. *J. Appl. Clin. Med. Phys.* **2016**, *17*, 61–74. https://doi.org/10.1120/jacmp.v17i3.5923.
22. Elamir, A.M.; Karalis, J.D.; Sanford, N.N.; Polanco, P.M.; Folkert, M.R.; Porembka, M.R.; Kazmi, S.A.; Maddipati, R.; Zeh, H.J.; Timmerman, R.D.; et al. Ablative Radiation Therapy in Oligometastatic Pancreatic Cancer to Delay Polyprogression, Limit Chemotherapy, and Improve Outcomes. *Int. J. Radiat. Oncol. Biol. Phys.* **2022**, *114*, 792–802. https://doi.org/10.1016/j.ijrobp.2022.07.019.
23. Byun, D.; Happersett, L.; Zhang, P.; Pei, X.; McBride, S.; Kollmeier, M.; Zelefsky, M. Variation in Interfractional Bladder Volume during Hypofractionated Radiation Therapy for Prostate Cancer. *Int. J. Radiat. Oncol.* **2016**, *96*, E614. https://doi.org/10.1016/j.ijrobp.2016.06.2168.
24. Jereczek-Fossa, B.A.; Fanetti, G.; Fodor, C.; Ciardo, D.; Santoro, L.; Francia, C.M.; Muto, M.; Surgo, A.; Zerini, D.; Marvaso, G.; et al. Salvage Stereotactic Body Radiotherapy for Isolated Lymph Node Recurrent Prostate Cancer: Single Institution Series of 94 Consecutive Patients and 124 Lymph Nodes. *Clin. Genitourin. Cancer* **2017**, *15*, e623–e632. https://doi.org/10.1016/j.clgc.2017.01.004.
25. Mancosu, P.; Clemente, S.; Landoni, V.; Ruggieri, R.; Alongi, F.; Scorsetti, M.; Stasi, M. SBRT for prostate cancer: Challenges and features from a physicist prospective. *Phys. Medica* **2016**, *32*, 479–484. https://doi.org/10.1016/j.ejmp.2016.03.011.
26. Otterson, M.F.; Sarr, M.G. Normal Physiology of Small Intestinal Motility. *Surg. Clin. N. Am.* **1993**, *73*, 1173–1192. https://doi.org/10.1016/s0039-6109(16)46186-4.
27. Grivel, M.-L.; Ruckebusch, Y. The propagation of segmental contractions along the small intestine. *J. Physiol.* **1972**, *227*, 611–625. https://doi.org/10.1113/jphysiol.1972.sp010050.
28. Karaus, M.; Wienbeck, M. Colonic motility in humans—A growing understanding. *Baillière's Clin. Gastroenterol.* **1991**, *5*, 453–478. https://doi.org/10.1016/0950-3528(91)90037-2.
29. Nuyttens, J.J.; Robertson, J.M.; Yan, D.; Martinez, A. The position and volume of the small bowel during adjuvant radiation therapy for rectal cancer. *Int. J. Radiat. Oncol.* **2001**, *51*, 1271–1280. https://doi.org/10.1016/s0360-3016(01)01804-1.
30. Cuccia, F.; Rigo, M.; Gurrera, D.; Nicosia, L.; Mazzola, R.; Figlia, V.; Giaj-Levra, N.; Ricchetti, F.; Attinà, G.; Pastorello, E.; et al. Mitigation on bowel loops daily variations by 1.5-T MR-guided daily-adaptive SBRT for abdomino-pelvic lymph-nodal oligometastases. *J. Cancer Res. Clin. Oncol.* **2021**, *147*, 3269–3277. https://doi.org/10.1007/s00432-021-03739-8.
31. Nuyttens, J.J.; Robertson, J.M.; Yan, D.; Martinez, A. The variability of the clinical target volume for rectal cancer due to internal organ motion during adjuvant treatment. *Int. J. Radiat. Oncol.* **2002**, *53*, 497–503. https://doi.org/10.1016/s0360-3016(02)02753-0.
32. Nijkamp, J.; de Jong, R.; Sonke, J.-J.; Remeijer, P.; van Vliet, C.; Marijnen, C. Target volume shape variation during hypo-fractionated preoperative irradiation of rectal cancer patients. *Radiother. Oncol.* **2009**, *92*, 202–209. https://doi.org/10.1016/j.radonc.2009.04.022.
33. Brierley, J.D.; Dawson, L.A.; Sampson, E.; Bayley, A.; Scott, S.; Moseley, J.L.; Craig, T.; Cummings, B.; Dinniwell, R.; Kim, J.J.; et al. Rectal Motion in Patients Receiving Preoperative Radiotherapy for Carcinoma of the Rectum. *Int. J. Radiat. Oncol.* **2011**, *80*, 97–102. https://doi.org/10.1016/j.ijrobp.2010.01.042.
34. Yamashita, H.; Takenaka, R.; Sakumi, A.; Haga, A.; Otomo, K.; Nakagawa, K. Analysis of motion of the rectum during preoperative intensity modulated radiation therapy for rectal cancer using cone-beam computed tomography. *Radiat. Oncol.* **2015**, *10*, 2. https://doi.org/10.1186/s13014-014-0311-6.
35. Chong, I.; Hawkins, M.A.; Hansen, V.; Thomas, K.; McNair, H.; O'Neill, B.; Aitken, A.; Tait, D. Quantification of Organ Motion During Chemoradiotherapy of Rectal Cancer Using Cone-Beam Computed Tomography. *Int. J. Radiat. Oncol.* **2011**, *81*, e431–e438. https://doi.org/10.1016/j.ijrobp.2011.04.060.

36. Elstrøm, U.V.; Muren, L.P.; Petersen, J.B.B.; Grau, C. Evaluation of image quality for different kV cone-beam CT acquisition and reconstruction methods in the head and neck region. *Acta Oncol.* **2011**, *50*, 908–917. https://doi.org/10.3109/0284186x.2011.590525.
37. Garayoa, J.; Castro, P. A study on image quality provided by a kilovoltage cone-beam computed tomography. *J. Appl. Clin. Med. Phys.* **2013**, *14*, 239–257. https://doi.org/10.1120/jacmp.v14i1.3888.
38. Grimmer, R.; Krause, J.; Karolczak, M.; Lapp, R.; Kachelriess, M. Assessment of spatial resolution in CT. In Proceedings of the 2008 IEEE Nuclear Science Symposium Conference Record, Dresden, Germany, 19–25 October 2008; pp. 5562–5566. https://doi.org/10.1109/nssmic.2008.4774508.
39. Keall, P.J.; Mageras, G.; Balter, J.M.; Emery, R.S.; Forster, K.M.; Jiang, S.B.; Kapatoes, J.M.; Low, D.A.; Murphy, M.J.; Murray, B.R.; et al. The management of respiratory motion in radiation oncology report of AAPM Task Group 76a). *Med. Phys.* **2006**, *33*, 3874–3900. https://doi.org/10.1118/1.2349696.
40. Yin, F.-F.; Wong, J.; Balter, J.; Benedict, S.; Bissonnette, J.-P.; Craig, T.; Dong, L.; Jaffray, D.; Jiang, S.; Kim, S.; et al. The Role of In-Room kV X-Ray Imaging for Patient Setup and Target Localization. 2009. Available online: https://www.aapm.org/pubs/reports/detail.asp?docid=104 (accessed on 8 September 2022). https://doi.org/10.37206/104.